State-to-state reaction rates: Ba+HF($v=0,1$)→BaF($v=0$–12)+H

J. Gary Pruett* and Richard N. Zare

Department of Chemistry, Columbia University, New York, New York 10027
(Received 24 October 1975)

The Ba+HF→BaF+H reaction has been studied under single-collision conditions as a function of the reagent and product vibration in order to obtain state-to-state reaction rates. Using a beam + gas arrangement, the HF is pumped by a pulsed HF laser and the BaF product distribution is determined from its laser-induced excitation spectrum. The BaF product is found to retain an average of 64% of the initial reactant vibrational excitation, and the distribution of product states for Ba+HF($v=1$) has a broad maximum shifted to $v=6$ from the value $v=1$ for Ba+HF($v=0$). The implications of these results on various proposed reaction surfaces are discussed.

I. INTRODUCTION

Although bulk reaction rates are nearly always the items of primary concern in the day-to-day applications of chemical kinetics, it is easily recognized that the task of measuring and cataloging all such macroscopic rates under all possible conditions of reagent mixtures, densities, and other pertinent parameters would be impossible. Early in the development of chemical kinetics, the value of microscopic rate constants of elementary reaction processes was recognized.[1] These more detailed building blocks were, and still are, very useful in gaining an understanding of a large number of chemical phenomena. This is especially true of those reactions that occur under conditions where the internal states of the reagents and products as a whole, or in parts, can be characterized by temperatures. Recently, much attention has been given to the study of individual reactive collisions, and their relation to bulk reaction kinetics.[2] For this purpose, it is necessary to perform kinetic studies under single-collision conditions, where collisional relaxation does not significantly degrade the observed product states. These studies show that the product state distributions usually cannot be described by temperatures, even within a particular degree of freedom, and the detailed reaction rates do not follow the laws of bulk kinetics. Consequently, it has become increasingly important to measure the individual rates at which the quantum states of the reactants evolve into the quantum states of the products during a single reactive encounter. A knowledge of these state-to-state reaction rates fully describes, in principle, the reactive system. It is hoped that as the rates measured more closely approximate state-to-state reaction rates, generalizations on the nature of the reaction dynamics will become evident.

Theoretical studies, of course, have approached kinetics from the opposite extreme, starting with the computation of state-to-state reaction rates, then making the appropriate averages in order to relate their calculations to experiments.[3] Unfortunately, this averaging process tends to obscure the predicted features of the reaction dynamics. This makes the comparison between theory and experiment less meaningful and hinders an assessment of the assumptions used in the computation. As experimental procedures develop for the determination of state-to-state reaction rates, more sensitive tests of theory should be possible.

Previous experimental work by many investigators has approached the determination of state-to-state reaction rates either by characterizing the internal and translational states of the products or the reactants.[4] Further discussion of some of these experiments is given in "Concluding Remarks." In particular, we have contributed to these efforts by using laser-induced fluorescence to probe the nascent internal states of a number of simple reaction systems.[5] Now it has been possible for us, by coupling laser-induced fluorescence detection of products with selective laser excitation of reagents, to obtain by means of one experiment detailed information on the relative vibronic state-to-state reaction rates. This is described here for one of a general class of simple bimolecular gas-phase exchange reactions.

We reported in 1973 the study of the crossed-beam reaction

$$\mathrm{Ba}+\mathrm{HF}\,(v=0) \xrightarrow{k(0,v)} \mathrm{BaF}\,(v)+\mathrm{H}\ , \tag{1}$$

in which the relative reaction rates for BaF in all different vibrational states were determined from its laser-induced excitation spectrum.[6] The specification of the reactant HF in the ground vibrational state occurred naturally from the Boltzmann population at room temperature. From this work it was concluded that the product internal states are not thermal and that an unusually small fraction of the total available energy appears as product vibration or rotation, i.e., the state-to-state rates for populating high energy internal states are unexpectedly small. We report here the study of this reaction with the further step of selectively preparing the HF molecule in the $v=1$ state prior to collision so that we can study the reaction

$$\mathrm{Ba}+\mathrm{HF}\,(v=1) \xrightarrow{k(1,v)} \mathrm{BaF}\,(v)+\mathrm{H}\ . \tag{2}$$

We find that the extra energy given to HF causes a significant but smaller than expected increase in the state-to-state reaction rates populating the high energy internal states of the BaF product. We describe here the experimental arrangement used in this study and present preliminary results for the Ba+HF reaction system.

II. EXPERIMENTAL

The experimental system is schematically shown in Fig. 1. It consists of three basic parts: (1) the molecular beam apparatus for carrying out the Ba+HF

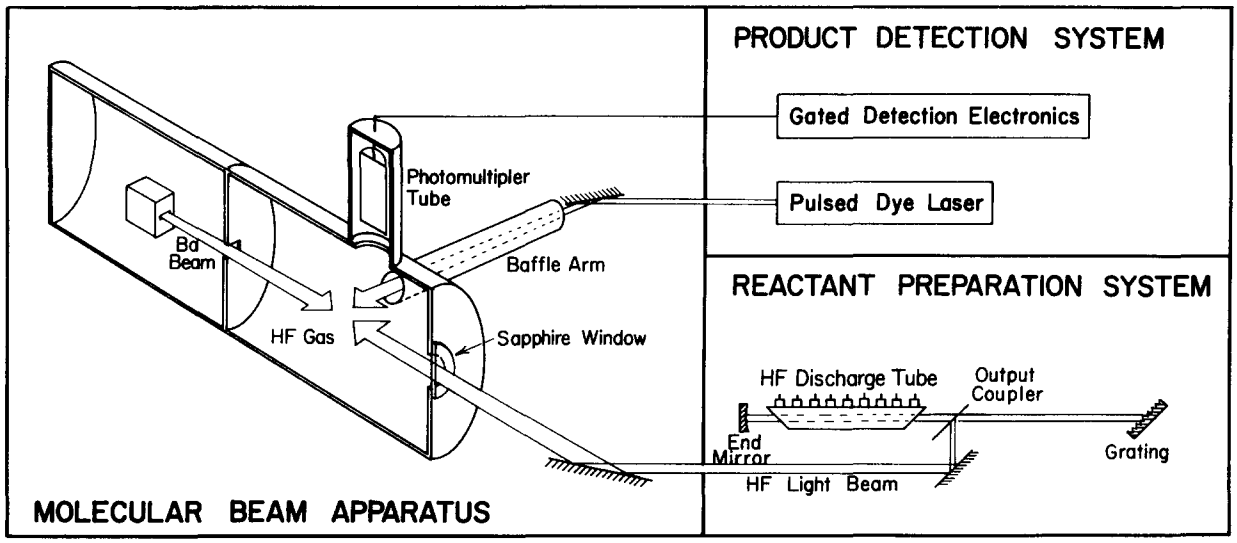

FIG. 1. Schematic of the experimental setup showing the molecular beam apparatus (cutaway drawing), the product detection system, and the reactant preparation system.

reaction under single-collision conditions; (2) the product detection system which probes the vibrational distribution of the BaF using laser-induced fluorescence; and (3) the reactant preparation system which excites a fraction of the HF molecules to the $v=1$ state using a pulsed HF laser. Systems similar to the first two parts have been used previously in our laboratory. The third part, namely the pulsed HF laser, was designed and constructed specially for this study. We describe each of these parts in turn.

A. Molecular beam apparatus

A molecular beam apparatus constructed in Professor P. Kusch's laboratory, Department of Physics, Columbia University, and kindly made available to us by Professor M. M. Hessel, Department of Physics, Fordham University, was modified to form the basic chambers of our vacuum system, shown in Fig. 1. Our apparatus consists of two brass chambers, each pumped by a single 4-in. oil diffusion pump and backed by separate mechanical pumps.

The oven chamber is water-cooled and houses a small beam oven heated by thermocoax wire and surrounded by nickel foil heat shields. The Ba metal (Atomergic Chemicals, >99% purity) was heated in the beam oven to 1100 °K (optical pyrometer reading) at which temperature the Ba metal has a vapor pressure of ~3 torr. This yields a beam flux of about 5×10^{16} atoms/cm^2-sec at the "fluorescence zone," defined approximately by the intersection volume of the Ba beam and visible laser beam, 12.5 cm from the oven slit. During operation, the oven chamber remained at a pressure below 2×10^{-6} torr.

A small rectangular slit, 2.0×0.3 cm, located 10 cm distant from the oven slit, serves to isolate the oven chamber from the reaction chamber and to collimate the Ba beam to a 6° horizontal and 0.8° vertical divergence. This isolation is necessary in order to prevent the relatively high densities of HF gas in the reaction chamber from reaching the hot Ba metal in the oven which could lead to interfering BaF molecules coming from the oven.

The HF gas is admitted directly to the reaction chamber through a stainless steel needle valve from a lecture bottle of HF (Matheson, >99.9% purity) which was immersed in a dry ice/acetone slush. The gas is purified before each run by pumping for a few seconds on the contents of the cold lecture bottle to remove SiF, and other high-vapor-pressure contaminants. The admitted gas makes many wall collisions at low pressure and room temperature before entering the reaction chamber. Under these conditions the concentration of HF dimers is negligible. The reaction chamber is typically filled during operation with 1×10^{-4} torr of HF gas. A liquid-nitrogen-cooled trap between the diffusion pump and the mechanical pump removes corrosive HF vapors.

The infrared pump laser is admitted coaxial with the Ba beam into the reaction chamber through a sapphire window, located sufficiently far away from the beam source so that no significant coating of the window occurs during an experiment. No exit port or baffling for the HF laser output is necessary since the HF laser pulse occurs several microseconds before the visible probe laser pulse, and the photomultiplier tube is relatively insensitive to the infrared light.

The dye laser probe beam is admitted into the reaction chamber through a 1-m-long baffle arm. The light passes through the fluorescence zone, 2.5 cm from the Ba beam entrance to the reaction chamber, and exits through another 1-m-long baffle arm. This construction is necessary because scattered light from the dye laser pulse nearly coincides, both temporally and spectrally, with the observed fluorescence. Therefore, scrupulous efforts must be made to prevent scattered light from the dye laser pulse from striking the photocathode of the photomultiplier tube. Design of the baffle arms will be discussed with the product detection system.

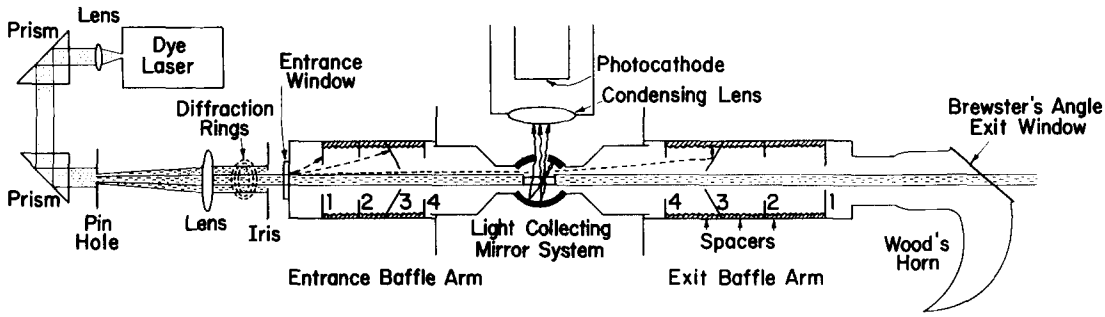

FIG. 2. Detailed view of the laser detection system showing the collimation of the dye laser beam and the collection of the fluorescent light.

B. Product detection system

A 300 kW pulsed nitrogen laser (Molectron Corp.) is used to pump a tunable dye laser (Molectron Corp., model DL300) operating without the intracavity etalon (typical bandwidth 0.2 Å). The BaF products are detected by exciting fluorescence in the $C^2\Pi_{1/2}-X^2\Sigma^+$ band system, lying near 5000 Å. For this purpose, 7-diethylamino-4-trifluoro-methylcoumarin dye (10^{-2} M) in p-dioxane is used as the laser medium. This dye solution gives a peak output at 5000 Å and is flat over the spectral range of interest (40 Å). The dye laser is operated at 20 pps, each pulse having a width of 10 nsec and a peak power of about 20 kW. The pulse-to-pulse amplitude stability is better than 5%.

The dye laser output is directed through a 10 cm focal length lens located near the laser output mirror and mounted on a translation stage, which is used to control the beam divergence (see Fig. 2). The light then passes through a pair of prisms, mounted in such a way as to provide nearly true horizontal and vertical translation of the beam. In addition, the mounts can adjust the vertical and/or horizontal inclination of the light beam. All adjustments are made with micrometer screws. The combination of lens and prism pair allows accurate alignment of the laser beam through the light baffle arms of the reaction chamber, pictured in Fig. 2. Immediately after the positioning prisms, the light enters a 1 mm pinhole that blocks the majority of the uncollimated fluorescent emission from the dye cell, and spatially defines the output beam. Approximately 1 m away, a second lens with long focal length, collimates the laser output to a nearly parallel beam 2 mm in diameter. A final iris external to the baffle assembly clips off the diffraction rings caused by the pinhole. The laser beam is now very well spatially defined, making it able to pass cleanly through the baffle arms.

After such stringent alignment of the laser beam, it might seem that very little additional effort would be required to keep stray light from entering the photomultiplier tube. However, a substantial amount of light is scattered at both the entrance and exit windows, even when they are carefully cleaned. In order to block such light from the view of the photomultiplier tube, the entrance and exit windows are placed at the ends of one-meter-long arms containing light baffles mounted coaxially along the arms.

Each arm contains four black anodized thin aluminum disks located at fixed distances along the baffle arm, the distances chosen to minimize light scattering, as indicated in Fig. 2. Black anodized spacer sleeves with threaded internal surfaces, are used to position each disk accurately and to absorb scattered light. Note that the third disk ($\frac{1}{4}$-in. diam hole) in each arm, numbering the disks from their respective windows, collimates the light directly scattered from each window so that all directly scattered light that passes through it also passes cleanly through the reaction zone and aperture number 4 ($\frac{3}{4}$-in. diam hole) of the opposite arm. Aperture 3 of the opposite arm intercepts this light but is tilted so as to reflect it away from the reaction zone. Aperture 1 ($\frac{1}{4}$-in. diam hole) and aperture 2 ($\frac{3}{4}$-in. diam hole) of either arm serve merely to isolate and absorb multiply scattered light. All of the extra surface area and confined air space cause only the delay of about 8 h in evacuating the molecular beam apparatus for an experimental run. A few extra black anodized sleeves and shields protect the immediate area around the photomultiplier tube and help remove the last traces of scattered light. After all these efforts, the scattered light level could be kept typically to about 10–20 photoelectrons per laser pulse (6×10^{14} photons). This rather ingenious design is primarily due to the efforts of Dr. Robert K. Sander, who plans to use this apparatus for future experiments.

Observation of the fluorescence is made by a photomultiplier tube (RCA 7265, 2-in. in diameter, S-20 photocathode) at right angles to both the Ba beam and the probe laser. Since normally the photomultiplier tube would only detect radiation emitted in the solid angle subtended by the photocathode, the tube is positioned as close to the fluorescence zone as practical (about 6 cm distant), and a short focal length, 4 cm, diam condensing lens is placed between the fluorescence zone and the photocathode to increase the solid angle observed.

In addition, a light-collecting mirror system, shown in Fig. 2, is installed surrounding the fluorescence zone except for the Ba beam and the probe laser entrance and exit apertures. This device is constructed from a burned-out home movie projector lamp (Model KP-GT, available from Lenmar Enterprises, Evanston, Illinois) which had apparently been designed to

collect the maximum amount of light from a straight coiled filament source and direct it towards the film image. By positioning the modified bulb structure so that the fluorescence zone is in the old filament region, light emitted in directions other than toward the photomultiplier tube is singly and multiply reflected onto the photocathode, as indicated in Fig. 2. This allows collection of approximately 50% of the total molecular fluorescence, corresponding to a factor of 5 improvement over previous light-collecting systems used in this laboratory.

The photomultiplier signal is averaged by a P. A. R. boxcar integrator model 162 main frame with either a 163 or 164 plug-in. The boxcar integrator receives its start pulse from a photodiode which senses the dye laser pulse. This procedure reduces the jitter between the boxcar gate and the fluorescence signal to less than 1 nsec. The boxcar integrator requires 30 nsec between the start pulse and the earliest obtainable gate opening. A corresponding pause in the signal pulse arrival is achieved using a delay line between the photomultiplier and the boxcar. To obtain a simple excitation spectrum the gate width on the 164 plug-in is chosen to be 50 nsec, which corresponds to three lifetimes of the BaF C states.[7] The laser is scanned at 5 Å/min and the boxcar is operated with an integrator time constant of 1 μsec, corresponding to an average of 100 laser pulses, or equivalently, about 0.5 Å.

The simple excitation spectrum may be taken with either the HF laser firing or not. For the HF laser on, a common pulse generator triggers both the HF laser and the nitrogen laser with a variable delay between the two start pulses. This delay is adjusted so that the HF laser fires before the nitrogen laser. The delay time is chosen so that the HF ($v=1$) molecules have sufficient time to react with Ba along the beam and so that the BaF products have time to enter the fluorescence zone. We find that the best excitation spectra are obtained using about a 50 μsec delay, although signal is observed from the Ba + HF ($v=1$) reaction from 0 to 80 μsec after the HF laser pulse.

In the latter stages of this study, the gated detection electronics and firing sequence was modified to permit the direct recording of the difference between the HF laser "on" excitation spectrum and the HF laser "off" excitation spectrum, called here the difference spectrum. This is achieved by utilizing the baseline sampling capability of the P. A. R. model 163 integrator plug-in. In this mode the plug-in acts as though it has two channels, a signal channel and a baseline channel, each of which have gates of exactly the same widths but separately variable time delays. The signal and baseline channels are sampled on alternate start pulses, and the difference is averaged by the plug-in. A Tektronix S-5 sampling head is used in conjunction with the model 163 plug-in to provide a 1 nsec gate which is open during the peak of the fluorescence signal. Although this gate width is 50 times shorter than that used in taking the simple excitation spectrum, the actual signal level is somewhat higher because the *average* voltage seen by the integrator during the gate duration (window) is larger for the short gate observing the peak of the fluorescence. In our application the signal and baseline gates are set to observe fluorescence at the same time delay with respect to the dye laser pulse. A pulse divider between the pulse generator and the HF laser causes the latter to fire on every other pulse of the dye laser. The signal channel receives the photomultiplier tube output for the HF laser on, and the baseline channel for the HF laser off, thus giving us directly the difference spectrum.

C. Reactant preparation system

A pulsed HF chemical laser was constructed using a pin electrode transverse discharge in a mixture of SF_6 (30 torr), H_2 (1 torr), and He (20 torr).[9] All gases are commercial grade and are continuously pumped through the laser tube by a Welch model 1375 pump, which is protected by a liquid-nitrogen-cooled trap. The cast acrylic laser tube is 82 cm long and has a 2.5 cm id. The pin electrodes are formed by 65 equally spaced 470 Ω resistors. Each resistor is sealed to the laser tube by an O-ring compressed between the wall of a socket machined in the tube and the resistor body. Discharge occurs across a 2 cm gap to a common aluminum ground strip. The discharge capacitor consists of 24 Sprague doorknob capacitors (500 pF, 30 kV) connected in parallel. It is charged through a current-limiting resistance network by a dc power supply (Del Electronics, model P5025-30-2) operated at 15 kV. The discharge capacitor is fired through a hydrogen thyratron (ITT, model F-43) by an external trigger.

The laser cavity (2 m long) is formed by a 10 m radius-of-curvature gold mirror at one end and a 300 grooves/mm grating (PTR Corp., model SF-800) operated in first order at the other end.[10] The laser tube is closed at both ends by Brewster's angle sapphire windows sealed by RTV to nylon adaptors. An uncoated sapphire flat is used as an output coupler for the HF laser radiation (see Fig. 1).

Figure 3 shows the laser output as a function of the grating angle illustrating the capability of forcing laser oscillation on a single selectable vibration–rotation transition. In this experiment we force laser action on the $P(2)$ line of the (1–0) transition. On this transition the HF laser delivers 110 μJ, as measured with a Scientech thermopile, in a 500 nsec pulse (200 W peak power). With a fresh tank of SF_6, the pulse-to-pulse amplitude stability is better than 5%. The laser output has a 5 mm spot size at a distance of 2 m from the output coupler. The 1–0 $P(2)$ line is chosen because room temperature HF has 26.4% of its molecules in the $v=0$, $J=2$ level (peak of the Boltzmann distribution), thus maximizing the fraction of molecules that can be selectively excited by the HF laser. The HF laser also operates superradiantly on high $P(J)$ lines of the 2–1 band, and some of this light also enters the reaction chamber. However, the superradiance pumps virtually no HF molecules since the lower levels of the 2–1 superradiance is not populated, either thermally or by the $P(2)$ 1–0 pumping line.

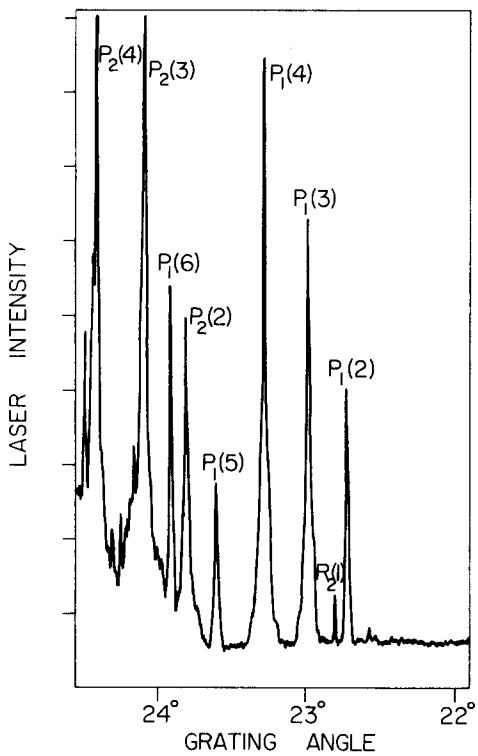

FIG. 3. HF laser intensity vs grating angle (measured from the laser axis to the grating normal). Unambiguous assignments are made by matching the calculated line positions with the observed output spectrum. The notation $P_1(2)$ signifies the $P(2)$ line of the $1 \rightarrow 0$ band, etc.

As will be discussed in the next section, the analysis of the difference spectrum requires a knowledge of the fraction of the observed BaF products that are formed by reaction with HF ($v=1$). This, in turn, requires a measurement of the fraction of HF molecules excited when irradiated by the HF laser. We denote this fraction by α, and disucss here our efforts to determine its value for the particular laser used in these experiments.

Unfortunately, the measurement of α is complicated by the fact that the laser bandwidth is narrower than the molecular absorption line. Moreover, the laser has mode structure[11] which further reduces the number of $v=0$, $J=2$ molecules that can absorb the laser output. Further complications are caused by saturation (nonlinear absorption) in which the laser power density varies with frequency within a single mode. Although some power broadening may occur, off-resonant pumping cannot be expected to simplify the determination of α. All these considerations indicate that α must be measured directly rather than calculated.

We follow a modified procedure to measure α, based on previous laser linewidth determinations.[11] A monel cell 10 cm in length with sapphire windows contains HF vapor at a pressure of 0.5 torr corresponding to its vapor pressure at -104 °C (cyclohexene slush). The intensity of the transmitted laser light is measured using an uncalibrated pyroelectric detector with the cell empty and the cell filled. In addition, the absolute power is measured using a thermopile. This information permits calculation of the average number of photons per pulse absorbed in the cell, which equals the average number of HF molecules excited by the laser. The total number of HF molecules is known from the pressure in the cell. Hence the fraction α is determined. For the 200 W pulsed HF laser, about 30% of each pulse is absorbed in the filled cell, and α is found to be 0.06 ± 0.01.

It should be stressed that this value of α only pertains to the conditions of the absorption cell. We must therefore estimate the value of α for the reaction chamber which has HF at a lower pressure (0.1 mtorr) and for which the HF laser power density is reduced due to the divergence of the laser beam and the somewhat lower powers used in the experiment. If the laser power is the same in the cell and in the reaction chamber, if no collisional relaxation occurs in the cell during the duration of the laser pulse, and if both the cell and reaction chamber are optically thin, then the same value of α would apply to both HF samples. Unfortunately these conditions are not met and we must consider the necessary corrections—corrections which only decrease α—to obtain a value of α for the reaction chamber.

When account is taken of the difference in power densities caused by the expansion of the spot size and the decreased total power used during experiments, we estimate that α is reduced by a factor of 6. In addition, the value of α in the reaction chamber should be reduced to account for collisional relaxation in the cell. Rather than attempting to make this correction, however, we take

$$\alpha \leq 0.01 \pm 0.005 \ , \tag{3}$$

as an upper bound, where the error estimate reflects the additional uncertainty caused by the power density correction. Although a more accurate upper bound to α or even an absolute value of α could be determined with additional work, we believe Eq. (3) suffices for this first study.

III. RESULTS AND DISCUSSION

A. Simple excitation spectrum

Figure 4 shows a low-sensitivity excitation spectrum obtained for BaF produced by reaction with only HF ($v=0$) and the spectrum obtained when the HF gas was irradiated by the HF laser output, resulting in a fractional contribution from BaF produced by reaction with HF ($v=1$). The peaks in the spectrum correspond to Q-branch heads formed at low J values of the $\Delta v=0$ sequence of the BaF $C^2\Pi_{1/2}$–$X^2\Sigma^+$ band system. Headless P and R branches are present which appear as an unresolved background. The Q-branch intensities can be subtracted from this background and related through Franck–Condon factors to the populations of the various nascent vibrational states of the BaF product as has been done in previous work. The resulting relative populations correspond to the rotationally and translationally averaged vibronic state-to-state reaction rates.

Since the fraction of BaF coming from vibrationally

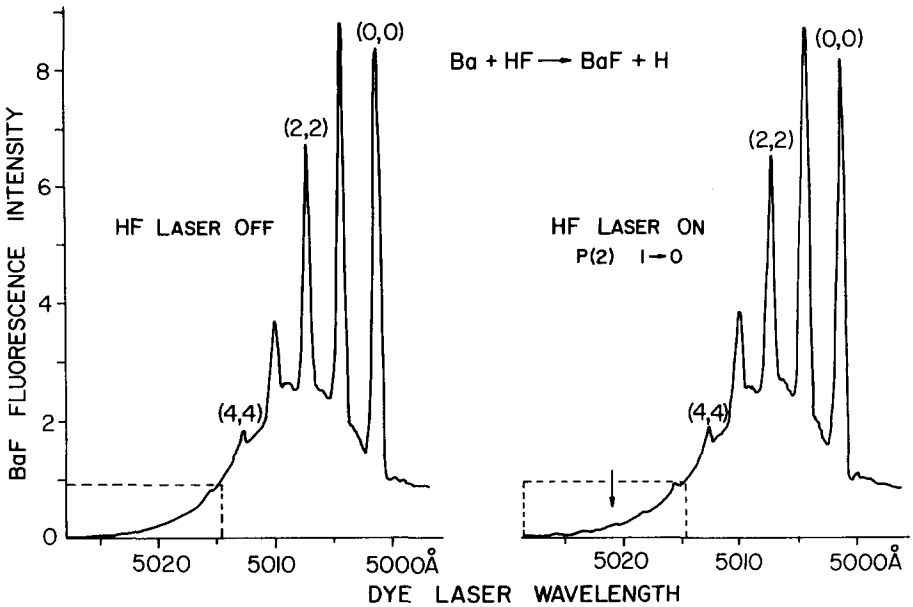

FIG. 4. Simple BaF excitation spectra (low sensitivity) for HF laser off and HF laser on. New band heads are just observable in the long wavelength tail of the HF laser on spectrum (see arrow).

excited reagents is small, the two spectra appear similar. However, closer examination of the long wavelength tail of the spectra shown in Fig. 5 reveals the appearance of new band heads of higher vibrational numbering in the $\Delta v = 0$ sequence. These band heads indicate that higher vibrational states of BaF are populated by Reaction (2). Their appearance strikingly illustrates the effect of adding a new mode of energy to one of the reagents of a reaction. It is obvious from Fig. 5 that vibrational states of BaF as high as $v = 11$ are being formed in the reaction of Ba with HF ($v = 1$). This represents an increase of almost a factor of two in the highest appreciably excited product state when comparing Reaction (1) with Reaction (2).

B. Difference spectrum

It is desirable to obtain an excitation spectrum characteristic of the products of Reaction (2) only. For this purpose, difference spectra are generated in three ways. First, the simple excitation spectra obtained when the HF laser is on or off are subtracted point by point, resulting in a difference spectrum of rather poor quality. Such a method is undesirable because of variations in experimental conditions within the time necessary to obtain the two separate spectra. Second, the visible probe laser is set to the wavelengths of each of the Q-branch peaks, one at a time, and the signal is integrated while blocking and unblocking the HF laser output at slow, 10 sec, intervals. This signal, tabulated for all peaks in Table I, corresponds to the difference spectrum at the Q-branch heads, and includes both the Q-branch head and any difference spectrum P-and R-branch background which underlies it. The data so obtained is fairly accurate, because of the long integration times used, but does not provide the necessary information of the Q-branch height above the P- and R-branch background. Third, the difference spectrum is directly obtained throughout the wavelength range as described in the experimental section. This spectrum, a portion of which is shown in Fig. 6,

TABLE I. Band head difference signals.

Band	Signal difference	Error
(3–3)	0.032	±0.020
(4–4)	0.035	±0.015
(5–5)	0.058	±0.012
(6–6)	0.053	±0.006
(7–7)	0.055	±0.006
(8–8)	0.053	±0.005
(9–9)	0.044	±0.004
(10–10)	0.026	±0.004
(11–11)	0.016	±0.004
(12–12)	0.011	±0.004

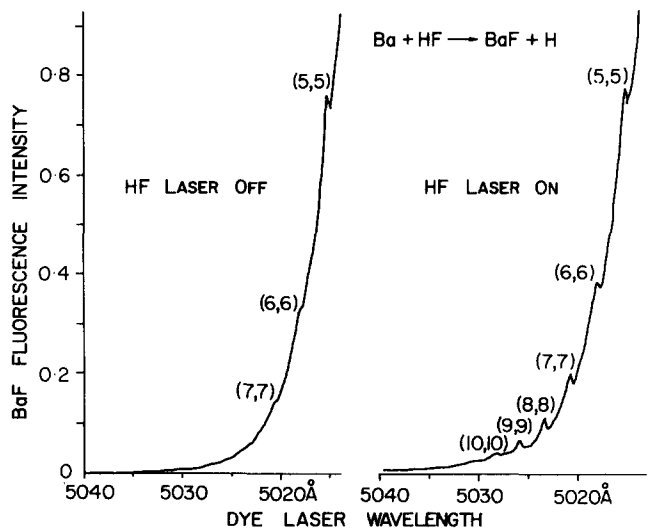

FIG. 5. Simple BaF excitation spectra (high sensitivity) for the long wavelength tail, enclosed by a dashed line box in Fig. 4, for HF laser off and HF laser on.

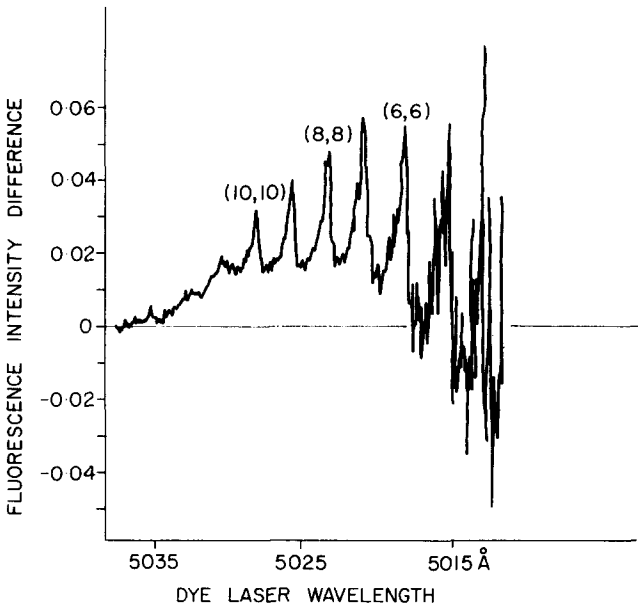

FIG. 6. Difference spectrum of the BaF reaction products. Notice that the noise increases rapidly at shorter wavelengths corresponding to the excitation of lower BaF v levels, caused by the increased contribution from reaction with HF ($v=0$). Note also that the signal makes excursions below the baseline, indicating excess subtraction of the signal component from the HF ($v=0$) reaction.

is degraded at the shorter wavelengths by all the problems of subtracting two very large signals to form a small difference. There is also a problem of dynamic range of the photomultiplier tube and boxcar integrator amplifier, which requires changes of scale during the scan of the dye laser to avoid overloading. Nevertheless, the difference spectrum is resolved to about $v=5$ on the short wavelength end, and provides the necessary heights of the Q-branch heads above the background.

C. Analysis of data

The difference spectrum, obtained by any of the above techniques, does not correspond to the pure excitation spectrum of BaF formed in the reaction of HF ($v=1$) with Ba. Unfortunately, *when one HF molecule is excited to the $v=1$ state, there is one less molecule to react from the $v=0$ state.* This causes a difficulty in relating the difference spectrum to the relative reaction rates, $k(1,v)$, for forming BaF (v) products by reaction with HF ($v=1$). The contribution to the "laser off" excitation spectrum from BaF products in the vibrational state v is given by

$$I_0(v) = C(v)k(0,v) \quad , \tag{3}$$

where $C(v)$ is a proportionality constant common to Reactions (1) and (2), the v dependence of which is just the Franck–Condon factor, $q_{v'=v,v''}$. Let β equal the fraction of detected BaF products that are produced by Reaction (2); then $(1-\beta)$ is that fraction for Reaction (1). The contribution to the "laser on" excitation spectrum from BaF(v) products is given by

$$I_L(v) = C(v)[\beta\, k(1,v) + (1-\beta)k(0,v)]. \tag{4}$$

Hence, the "laser on" spectrum corresponds to a laser off spectrum of reduced intensity superimposed on the pure excitation spectrum of Reaction (2). The contribution of BaF(v) to the difference spectrum is

$$\begin{aligned}\Delta I(v) &= I_L(v) - I_0(v) \\ &= C(v)\,\beta[k(1,v) - k(0,v)] \quad .\end{aligned} \tag{5}$$

Thus the difference spectrum is the excitation spectrum of Reaction (2) *plus* a negative contribution caused by the loss of reaction from the HF ($v=0$) reactants which were transformed to HF ($v=1$) reactants by the HF laser pulse. Since $k(0,v)$ is determined up to a proportionality constant by the "laser off" spectrum [see Eq. (3)], we can find $k(1,v)$ up to the same proportionality constant from the difference spectrum by

$$k(1,v) = C^{-1}(v)[\Delta I(v)/\beta + I_0(v)] \quad , \tag{6}$$

and this analysis requires a knowledge of the fraction β of the total products observed that come from reactions of vibrationally excited reagents.

It is instructive for the determination of β to consider a few limiting cases. Let us assume that the total rates of Reactions (1) and (2), are identical, i.e.,

$$\sum_v k(0,v) = \sum_v k(1,v) \quad . \tag{7}$$

This might be a fair approximation because Reaction (1) is already exothermic with a sizeable cross section and it is improbable that added energy would increase the total reaction rate significantly. Then, if the vibrational distributions of BaF from Eqs. (1) and (2) were identical, i.e., $k(0,v)=k(1,v)$, there would be no difference spectrum. If, however, the vibrational distributions were different, the difference spectrum would have both positive and negative peaks, and the total area under the curve would be equal to zero.

Only one clue to the value of β is obtainable from the difference spectrum of this work. Figures 4 and 5 show that there are essentially no BaF($v \geq 6$) products formed by reaction with HF($v=0$). Therefore, essentially all contributions to the difference spectrum for $v \geq 6$ are positive. If we continue the assumption of a constant total reaction rate [see Eq. (7)], then the area under the difference spectrum for $v \geq 6$ can be compared to the area under the "laser off" spectrum to find a *minimum* value of β. By comparing the properly normalized area under the curve of Fig. 6 for $v \geq 6$ with the total area under the "laser off" spectrum of Fig. 4, we estimate that

$$\beta \geq 0.01 \pm 0.005 \quad . \tag{8}$$

We note that if vibrational excitation of HF increases the total rate of Reaction (2) over Reaction (1), this lower bound for β would decrease, but not necessarily by a corresponding amount.

It is possible to make another independent estimate of β by utilizing the estimated initial fraction α of excited HF calculated previously to be about 1.0% (see experimental section). Note this value for α cannot be directly used as β since a very complicated dilution of the vibrationally excited HF occurs prior to reaction and detection of the reaction product. This is caused

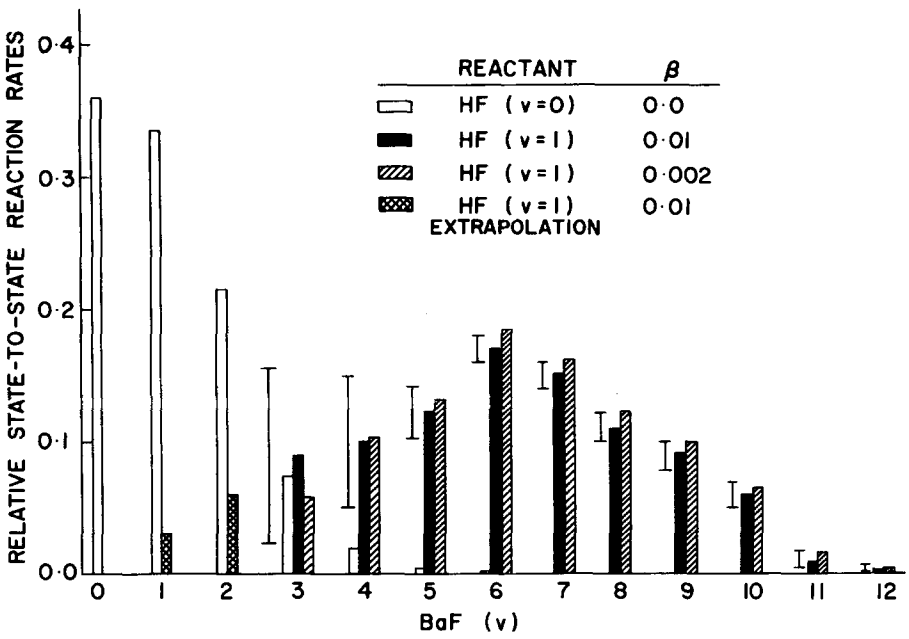

FIG. 7. Bar graph showing the state-to-state reaction rates for $Ba + HF(v=0,1) \rightarrow BaF(v) + H$. Two calculations for $Ba + HF(v=1)$ are displayed, corresponding to two different possible fractions of HF vibrational excitation. The error bars indicate the uncertainty in the $k(1,v)$ ratio.

by the random velocity vectors of the HF molecules, and the spatially confined natures of the Ba beam, the HF laser irradiation zone, and the dye laser probe zone. For the particular geometry used in this experiment, an exact conversion from α to β seems an unpromising task, considering the lack of precision already present in the value of α. Instead we choose to make an approximate estimate of β from α which should have sufficient precision to permit a comparison with the value of β in Eq. (8). This calculation proceeds by making the following geometrical assumptions: (1) the HF laser beam diameter is approximately one-half that of the Ba beam width but greater than its height; (2) the BaF produced travels with a single laboratory velocity along the center-of-mass velocity vector, which in turn is essentially in the direction of the Ba beam; and (3) no BaF is produced by either reaction with $v=1$ or $v=0$ HF until the Ba enters the scattering chamber, 2.5 cm before the probe laser zone. Condition 1 results in an automatic decrease by a factor of 2 of α. Condition 2 causes the BaF products to expand in the same manner as the Ba beam, with their density falling off with distance as $1/r^2$, r being measured from the oven orifice. However, since the probe laser is insensitive to expansion in the horizontal plane, a $1/r$ rather than a $1/r^2$ is used as an approximation of the product density falloff with distance. Condition 3 defines the range of time and spatial position within which the detected BaF was produced. This allows a simple integration over possible product origins, weighted by their density falloff with distance from the observation zone. We find

$$\beta = 0.2\,\alpha = 0.002 \ . \tag{9}$$

Although the estimate of β in Eq. (8) is at least twice as large as that in Eq. (9), we feel that the uncertainties in carrying out the estimate of β in Eq. (9) are sufficiently large that it is reasonable to assume that the total rates for Reactions (1) and (2) are equal [see Eq. (7)]. We use both values of β in reducing the difference spectrum to state-to-state reaction rates, and show that the results are rather insensitive to a decrease in the value of β, and fairly insensitive to an increase in its value. Hence, our analysis of the data becomes insensitive to the validity of Eq. (7).

Equations (3) and (6) are evaluated for the relative state-to-state reaction rates $k(0,v)$ and $k(1,v)$ by using the Franck–Condon factors of Ref. 6 to remove the v dependence of the proportionality constant $C(v)$, and using Fig. 6 and Table I, Eq. (8), and Fig. 4 for the values of $\Delta I(v)$, β, and $I_0(v)$, respectively. These rates are normalized to unity. They are displayed in Fig. 7 and listed in Table II. Also shown in Fig. 7 are the results for $\beta = 0.002$ [see Eq. (9)], as well as extrapolated values for $k(1,0-2)$. The error bars in Fig. 7 increase towards low values of v, reflecting

TABLE II. Relative state-to-state reaction rates normalized to unity.

BaF(v)	$k(0,v)$	$k(1,v)$
0	0.360 ± 0.02	0.0[a]
1	0.335 ± 0.02	0.03[a]
2	0.215 ± 0.02	0.06[a]
3	0.073 ± 0.01	0.09 ± 0.07
4	0.018 ± 0.005	0.10 ± 0.05
5	0.005 ± 0.002	0.12 ± 0.02
6	0.002 ± 0.001	0.17 ± 0.01
7	0.0005 ± 0.0005	0.15 ± 0.01
8	···	0.11 ± 0.01
9	···	0.09 ± 0.01
10	···	0.06 ± 0.01
11	···	0.01 ± 0.005
12	···	0.003 ± 0.003

[a]Extrapolated values using a linear function that passes through the origin and $k(1,3)$.

the growing uncertainty in measuring the difference of less than 2% between two large signals for vibrational levels below BaF($v=6$). The two bar graphs for $k(1,v)$ are very similar, demonstrating the insensitivity of the qualitative features to a decrease of β below 0.01. It can be seen that the $k(1,v)$ show a broad maximum between $v=5$ and $v=8$. For larger values of β it might be argued that the BaF production in $v \leq 3$ rises above the production for $v \geq 5$, thus causing a qualitative change in the $k(1,v)$ distribution. We exclude this possibility, however, because it requires β to be greater than the value of α estimated in the experimental section.

An attempt was made by Dr. Gregory P. Smith of laboratory to fit various portions of the difference spectrum (Fig. 6) to assumed rotational Boltzmann distributions in order to estimate rotationally resolved reaction rates. The results were rather inconclusive because of the quality of the spectrum and the possibility of optical pumping. Nevertheless, the results indicate a rotational state distribution with a mean energy at least that for Ba + HF($v=0$), as determined in previous work.

D. Concluding remarks

It seems to be the rule that a large fraction of the energy available in an exothermic exchange reaction appears as product vibration.[12] This experimental generalization has received support from various trajectory calculations, especially those for reactions on LEPS surfaces characterized as having attractive or mixed energy release. In particular, the mass combination H + HL → HH + L (H = heavy, L = light) is known to favor mixed energy release, which generally results in substantial vibrational excitation of the products.[13] A counterexample to the above is the reaction of this study, Ba + FH → BaF + H which is of the H + HL → HH + L class of reactions and which has been found to produce very low product vibrational excitation.[6] Of the energy available to the products (12.6 kcal/mole), an average of only 12% appears as vibration, 13% as rotation, and 75% as product translation. These results suggest that in terms of previous LEPS-type surfaces studied, the Ba + HF reaction occurs on a highly repulsive surface where mixed energy release plays little role. Alternatively, Duff and Truhlar[14] have proposed that mixed energy release could still occur, but that the curvature of the minimum energy path preferentially directs released energy into product translation. Their own results, however, indicate that for this mass combination, the effect of curvature is greatly diminished.

In this study we have investigated the BaF vibrational distribution when the HF is excited from the $v=0$ to the $v=1$ state. This reactant excitation energy (11.0 kcal/mole) corresponds to almost nine vibrational quanta of the BaF product, and has the potential of "triggering" an even larger release of reaction exothermicity into product vibration. Indeed, in other reaction systems it has been found generally that excess reactant vibration is adiabatically transferred as extra product vibration with almost complete retention.[15,16] Instead, the results shown in Fig. 7 contradict this expectation, namely, the average fraction of excess reactant vibration appearing as product vibration is 0.57—much less than it would be possible to obtain.

This fraction is found in the following manner. The average vibrational energy of BaF is calculated for Reactions (1) and (2). The difference between these averages is then divided by the HF excitation energy. In carrying out this calculation for Ba + HF($v=1$), it is assumed the state-to-state reaction rates for producing BaF ($v \leq 2$) decreases linearly to zero from the value at BaF ($v=3$). If this procedure underestimates the population of these low vibrational states, then the effect will be to decrease even further the fraction of energy appearing in product vibration. While this fraction may be less than expected, the extra 11.0 kcal/mole of energy added to the reactant vibration are partioned in the products in a totally different way than are the original 12.6 kcal/mole of reactant energy and reaction exothermicity. Viewed alternatively, the *total* available energy that is partitioned into product vibration changes from 12% to 33% in going from Ba + HF($v=0$) to Ba + HF($v=1$).

Consideration of the average disposal of energy to various product modes is of interest in comparison with previous generalizations, but we are in a unique position to discuss the shapes of the state-to-state rate distributions and their possible implications on the properties of the reaction dynamics. Comparison of $k(0,v)$ and $k(1,v)$ in Table II shows that $k(0,v)$ has appreciable value only over a limited range of product vibrational states, whereas $k(1,v)$ is spread out over a much larger range. This implies that the HF($v=1$) vibrational energy does not simply map in a linear manner into BaF vibrational energy, as this would result in a simple shift in the $k(0,v)$ distribution. Previous infrared chemiluminscence results for F + HCl and Cl + H_2 show related behavior.[15] It is of course possible to analyze state-to-state reaction rates by an information-theoretic approach.[17] Although vibrational surprisal plots have been prepared, they are nonlinear in form and their smoothness only suggests the internal consistency of the present data.

It is interesting to speculate about the form of the observed state-to-state reaction rates. For a reaction surface with a simple smooth topography, the effect of vibrational energization is to cause the product to enter the exit valley from the side, rather than to follow the minimum energy path. There are then two types of possibilities.[15] First, the reaction occurs early in the collision while the reagent bond is extended, causing the trajectory to "cut the corner" in going from the entrance valley to the exit valley at larger internuclear distances than the minimum energy path. This type of trajectory preferentially leads to product vibration. Second, the reaction occurs late in the collision if the trajectory "misses" the exit valley on its initial pass along the surface. In this case, the trajectory runs deeply into the corner of the reaction surface and is "pushed" by the repulsive surface back into the reaction channel. This type of trajectory tends to give lower product vibration. The key ingredient for determining the amount of product vibration in

either of these cases is the direction of the force felt by the product nuclei when the energy is released. Entering the exit valley from the side tends to release energy into the product bond coordinate, while a "perpendicular" path through the reaction channel tends to release the energy into the "separation coordinate," giving high product translation.

It appears that there are two choices for the potential surface which could explain the present results. If the surface is of the smooth topography discussed above, then the large fraction of energy appearing as product translation, the moderate fraction of HF vibration appearing as BaF vibration, and the broad distribution of $k(1,v)$ values seem to argue that the surface is highly repulsive, i.e., the energy is released after the H atom has already moved a distance away from the newly formed BaF bond, and the topology of the corner of the surface is broad and shallow, allowing entry into the product valley at a wide range of internuclear separations. The type of surface, in Duff and Truhlar's classification,[14] would have almost no minimum energy path curvature in the region of energy release.

However, there is reason to wonder whether the reaction surface is well behaved because the Ba+HF reaction involves a "switch" from covalent to ionic bonding. Consequently, the surface may have special topological features that could account for the observed reaction dynamics. Indeed, Polanyi[13] has suggested that the results could be explained by an exceptionally narrow reaction channel which forces the trajectories into a perpendicular reaction path. A surface of this type has already been proposed for the K+HBr reaction which also involves an abrupt covalent to ionic transformation.[18,19] This surface has a narrow reaction channel located early in the exit valley. In order to explain the present results, reactions on such a surface must follow nearly perpendicular trajectories. This is entirely possible, however, since the HF vibrational period is short compared to the collision time, so that all trajectories have a rapidly oscillating perpendicular component, i.e., a component along the HF bond for fixed BaF bond distance. Thus, for ground vibrational state reagents, a perpendicular reaction path through the narrow channel results in low product vibration. For vibrationally excited reagents, the reaction path is still perpendicular, but the trajectory can enter the reaction channel earlier and a little more from the side, so that the repulsive force experienced by the atoms would be less perpendicularly directed, resulting in modest product vibration.

Although we prefer this last explanation as more reasonable on chemical grounds, we cannot at this time distinguish between the two possible reaction surfaces. However, the detailed information now avialable for the Ba+HF reaction should make it possible, with the help of surface and trajectory calculations, to gain insight into the reaction dynamics for this class of reactions. Such future calculations can be directly compared to the state-to-state reaction rates becoming available through the experimental technique described here.

ACKNOWLEDGMENTS

We thank Dr. Robert K. Sander for his valuable assistence in the construction of the molecular beam apparatus and lightbaffling system. We are also grateful to Dr. Gregory P. Smith for his computer calculation on the BaF product rotational distribution. This work was supported in part by the Air Force Office of Scientific Research under grant AFOSR-73-2551C and by the National Science Foundation under grant NSF-MPS-72-04333 AO3.

*Present address: Department of Chemistry, University of Pennsylvania, Philadelphia, PA 19174.

[1]S. W. Benson, *The Foundations of Chemical Kinetics* (McGraw–Hill, New York, 1960).
[2]R. D. Levine and R. B. Bernstein, *Molecular Reaction Dynamics* (Oxford University, New York, 1974).
[3]D. L. Bunker, *Theory of Elementary Gas Reaction Rates* (Pergamon, Oxford, 1966).
[4]M. J. Berry, *Molecular Energy Transfer*, edited by J. Jortner and R. D. Levine (Wiley, New York, in press).
[5]R. N. Zare and P. J. Dagdigian, Science **185**, 739 (1974).
[6]H. W. Cruse, P. J. Dagdigian, and R. N. Zare, Faraday Discuss. Chem. Soc. **55**, 277 (1973).
[7]P. J. Dagdigian, H. W. Cruse, and R. N. Zare, J. Chem. Phys. **60**, 2330 (1974).
[8]M. C. Lin and W. H. Green, J. Chem. Phys. **53**, 3383 (1970).
[9]O. R. Wood and T. Y. Chang, Appl. Phys. Lett. **20**, 77 (1972).
[10]W. H. Green and M. C. Lin, J. Chem. Phys. **54**, 3222 (1971).
[11]L. M. Peterson, C. B. Arnold, and G. H. Lindquist, Appl. Phys. Lett. **24**, 615 (1974).
[12]J. C. Polanyi, J. Chem. Phys. **31**, 1338 (1959); J. C. Polanyi, Acc. Chem. Res. **5**, 161 (1973).
[13]J. C. Polanyi, Faraday Discuss. Chem. Soc. **55**, 389 (1973).
[14]J. W. Duff and D. G. Truhlar, J. Chem. Phys. **62**, 2477 (1975).
[15]A. M. G. Ding, L. J. Kirsch, D. S. Perry, J. C. Polanyi, and J. L. Shreiber, Faraday Discuss. Chem. Soc. **55**, 252 (1973).
[16]D. S. Perry, J. C. Polanyi, and C. W. Wilson, Jr., Chem. Phys. **3**, 317 (1974).
[17]R. B. Bernstein and R. D. Levine, "Role of Energy in Reactive Molecular Scattering: An Information–Theoretic Approach," *Advances in Atomic and Molecular Physics*, edited by D. R. Bates (Academic, New York, 1975), Vol. II.
[18]R. J. Susplinskas and J. Ross, J. Chem. Phys. **47**, 321 (1967).
[19]A. C. Roach, Chem. Phys. Lett. **6**, 389 (1970).